

Re-visiting the structural and glacial history of the Shackleton Glacier region of the Transantarctic Mountains, Antarctica

David H. Elliot

To cite this article: David H. Elliot (2022): Re-visiting the structural and glacial history of the Shackleton Glacier region of the Transantarctic Mountains, Antarctica, New Zealand Journal of Geology and Geophysics, DOI: [10.1080/00288306.2022.2114505](https://doi.org/10.1080/00288306.2022.2114505)

To link to this article: <https://doi.org/10.1080/00288306.2022.2114505>



© 2022 The Author(s). Published by Informa UK Limited, trading as Taylor & Francis Group



Published online: 24 Aug 2022.



Submit your article to this journal



Article views: 460



View related articles



View Crossmark data





Re-visiting the structural and glacial history of the Shackleton Glacier region of the Transantarctic Mountains, Antarctica

David H. Elliot

School of Earth Sciences and Byrd Polar and Climate Research Center, Ohio State University, Columbus, OH, USA

ABSTRACT

Only at Cape Surprise, central Transantarctic Mountains, is there exposed stratigraphic evidence for major offset along the range front, which marks a major boundary in Antarctica. Several faults parallel to the range front have been identified in the Devonian to Triassic Gondwana strata in the hinterland. Analysis of the stratigraphy based on field observations and the United States Geological Survey (USGS) aerial photographs, in conjunction with USGS topographic sheets and satellite-derived elevation measurements, suggests an array of faults with varying orientations and displacements. Fault offsets range up to an estimated 850 metres. No additional range-parallel faults have been identified and no clear pattern of faulting is evident in the hinterland of the frontal escarpment. Faulting may date from the time of slow uplift during the Cretaceous as well as the more rapid Cenozoic uplift of the range. Only a few faults in the hinterland can be allied with the frontal fault system. Cenozoic uplift and associated denudation was accompanied by glaciation of Antarctica, which is documented by Sirius Group strata. These deposits, which pre-date today's polar landscape, are older than mid Miocene, and in part may date from the earliest stages of warm-based glaciation in the early Oligocene.

ARTICLE HISTORY

Received 14 May 2022
Accepted 12 August 2022

HANDLING EDITOR

James Scott

KEYWORDS

Transantarctic Mountains;
Beacon stratigraphy;
Cenozoic; faults; Sirius
Group; glaciation

Introduction

The Transantarctic Mountains (TAM) mark the geographic boundary between East and West Antarctica (Figure 1), however, the geological boundary is now interpreted, on geophysical grounds (Tinto 2019), to be located within the Ross embayment (Ross Ice Shelf-Ross Sea region) (Figure 1). The geological boundary is a fundamental feature of Antarctic geology, separating thin extended crust of West Antarctica, which consists principally of Lower Palaeozoic to Upper Mesozoic orogenic belts, from the Neoproterozoic to Lower Ordovician Ross orogenic belt and its hinterland of the East Antarctic craton. The crust on the TAM side of the geological boundary is thinned, like that under the eastern Ross Ice Shelf, but its thickness increases rapidly under the TAM to normal crustal values. This lithospheric boundary was established in the Neoproterozoic (Dalziel 1997) and was a critical feature during the break-up of Gondwana in the Early Jurassic (e.g. Dalziel and Lawver 2001), when the Gondwana active margin belts alongside the East Antarctic craton were dismembered and re-arranged. By about 100 Ma the various continental blocks of West Antarctica were in their current relative positions (Grunow et al. 1987, 1991). Extension in the Ross Sea sector was initiated in late Cretaceous time (Siddoway

et al. 2004, Siddoway 2008) and continued during the Cenozoic along with uplift and denudation of the Transantarctic Mountains (e.g. Fitzgerald 2002). The near synchronicity of the initiation of uplift along the length of the TAM implies that extension of the East Antarctic cratonic rocks and the bounding Ross Orogenic belt, now within the Ross embayment, must mainly, if not entirely, predate TAM uplift and have occurred in Late Cretaceous to Early Eocene time.

The TAM was recognised to be the result of major faulting by David and Priestley (1914) who described it as a horst but the first direct stratigraphic evidence of displacement came with discovery of Permian Beacon strata at Cape Surprise (Figure 2) (Barrett 1965). Offset of the strata was estimated to be as much as 4 km. The only other stratigraphic evidence comes from probable Devonian strata recovered in an offshore drill core at Cape Roberts, southern Victoria Land (Figure 1), which suggests about 3 km of offset (Cape Roberts Science Team 2000). The various explanations for the juxtaposition of the uplifted TAM and the extended West Antarctic Rift System (WARS) are based on geological, seismic and gravity studies. Many authors link uplift and extension directly (e.g. Fitzgerald 1992; van Wijk et al. 2008, and references therein); others suggest strike-slip faulting rather than normal

CONTACT David H. Elliot elliott.1@osu.edu

Supplemental data for this article can be accessed online at <https://doi.org/10.1080/00288306.2022.2114505>.

© 2022 The Author(s). Published by Informa UK Limited, trading as Taylor & Francis Group
This is an Open Access article distributed under the terms of the Creative Commons Attribution-NonCommercial-NoDerivatives License (<http://creativecommons.org/licenses/by-nc-nd/4.0/>), which permits non-commercial re-use, distribution, and reproduction in any medium, provided the original work is properly cited, and is not altered, transformed, or built upon in any way.

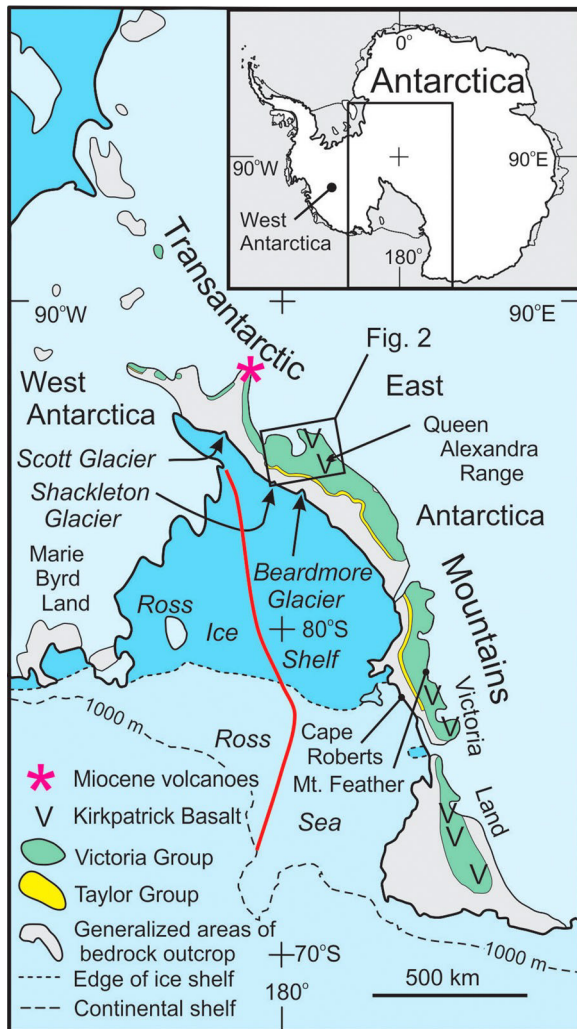


Figure 1. Location map for Antarctica. Red line is the approximate boundary between East and West Antarctic crust (Tinto 2019).

faulting (e.g. ten Brink et al. 1997). An alternate proposal is that flexural uplift accompanied by glacial erosion under polar conditions, in which the absence of freeze-thaw mechanisms leads to very slow rates of erosion compared with lower elevations at warmer temperatures and with ice at the pressure melting point, accounts for the high elevation of the TAM (Stern et al. 2005). Crustal thickness contrasts between the TAM and WARS together with numerical modeling and geological constraints have been interpreted to suggest the TAM is a marginal remnant of a Mesozoic-age continental plateau formerly located in West Antarctica (e.g. Bialas et al. 2007). Strain partitioning across the TAM and WARS, with detachments rooted in the mantle, has been suggested as a mechanism to explain the uplift (Fitzgerald and Baldwin 1997). A consensus is developing that flexural uplift and thermal buoyancy are significant factors in the formation of the TAM (e.g. Shen et al. 2018; Emry et al. 2020). Lastly, Granot and Dymant (2018) suggest the changing kinematic regimes of the TAM uplift along its

length is related to the Neogene history of the merging of East and West Antarctica as a single plate.

The importance of the uplift history of the TAM to the climate and glacial history of Antarctica (Barrett 1996) spurred apatite fission track and (U-Th)/He thermochronological studies of the Lower Palaeozoic granitoids of the Ross Orogen. The investigations between southern Victoria Land and Scott Glacier (Gleadow and Fitzgerald 1987; Fitzgerald 1994; Fitzgerald and Stump 1997; Fitzgerald et al. 2006; Guo et al. 2021; He et al. 2021) are the most relevant to the region of interest, which is the Shackleton Glacier area (Miller et al. 2010). They demonstrated the Cenozoic age of major uplift/denudation, and the location and pattern of faults offsetting basement rocks. Although the onset of uplift began at about 55 Ma in southern Victoria Land, elsewhere it was somewhat younger and in the Shackleton Glacier region it began at about 40 Ma. In the Queen Alexandra Range, about 160 km northwest of the Shackleton Glacier, (U-Th)/He thermochronology suggests onset of the most rapid uplift and denudation occurred there at about 35 Ma (He et al. 2021).

The aim of this paper on the geology of the Shackleton Glacier region, which was prompted by submission of maps for the SCAR (Scientific Committee on Antarctic Research) digital geological map of Antarctica (Cox and Smith Lyttle 2022), is to evaluate the major structures displacing the Gondwana succession in the hinterland of the TAM escarpment and their relationship to the inferred frontal fault system. In addition, the relationship of the glaciogenic Sirius Group beds to the structural evolution of the Shackleton Glacier region is re-examined and aspects of palaeotopography noted.

Regional geology

The geology of the central Transantarctic Mountains is relatively simple: pre-Devonian basement rocks are overlain by undeformed Devonian to Lower Jurassic Gondwana strata (Beacon Supergroup and Ferrar Group of Antarctica) and Cenozoic glacial deposits (Figure 2). The basement comprises low-grade metasedimentary and metagneous rocks intruded by Neoproterozoic to Ordovician granitoids (Goodge 2020). Erosion of the basement rocks formed the Kukri Erosion Surface (Isbell 1999) on which the Gondwana succession accumulated (Figure 3) (Barrett 1991; Elliot 2013). Quartzose sandstones (Alexandra Formation) form scattered thin successions of strata assigned a Devonian age, which is based on lithologic correlation with beds in southern Victoria Land (Bradshaw 2013). Permian glacial strata (Pagoda Formation) overlie a younger erosion surface, the Maya Erosion Surface, which truncates all older rocks. Pagoda strata are succeeded by post-glacial shales (Mackellar Formation), deltaic sandstones of the Fairchild Formation and then the coal-bearing Buckley

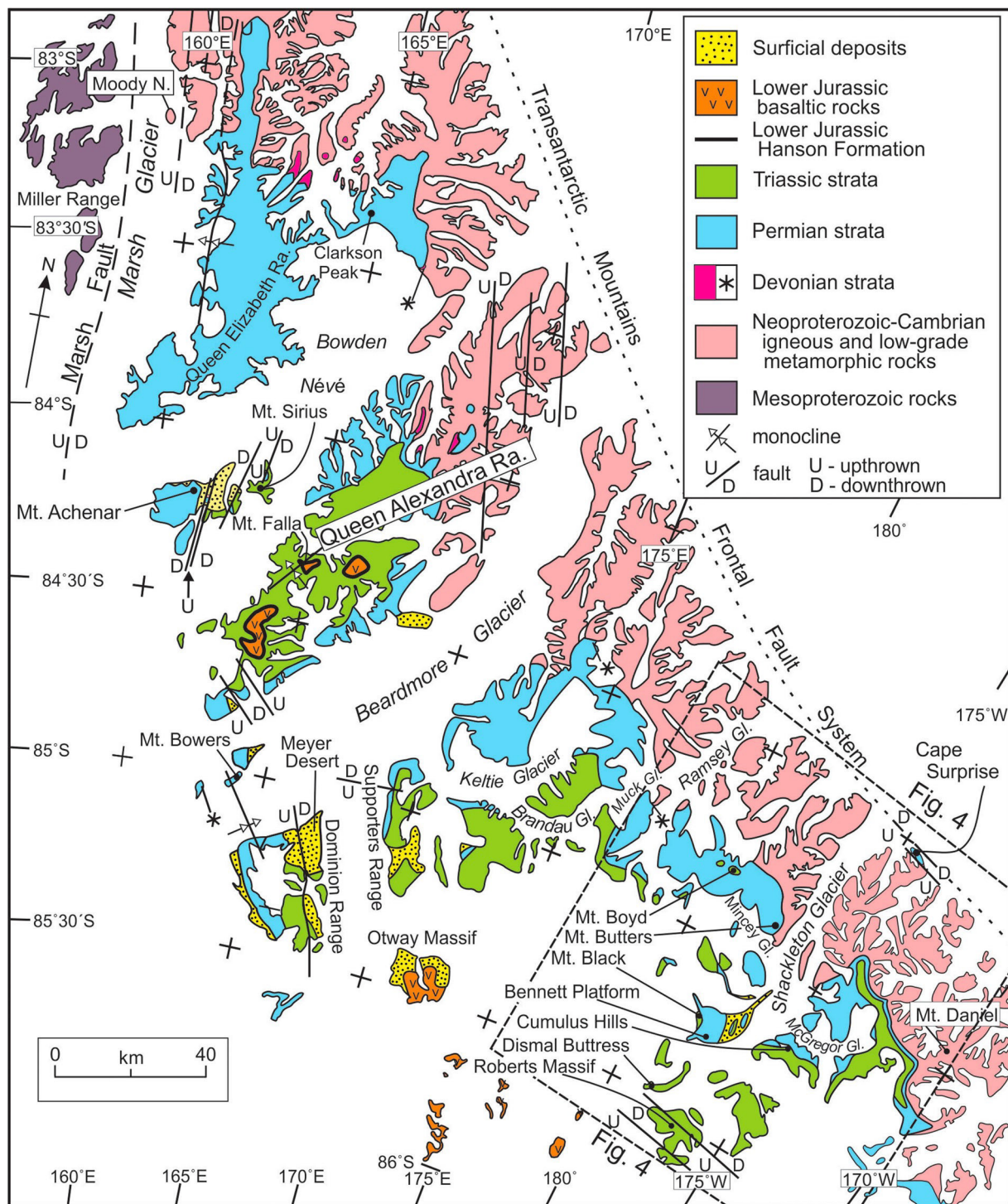


Figure 2. Geological sketch map of the central Transantarctic Mountains. Lower Jurassic Ferrar Dolerite sills are co-extensive with Permian and Triassic strata. The '*' indicates locations of Devonian strata too small to illustrate at the map scale. Illustrated faults and monoclines are from Barrett et al. (1970), Barrett and Elliot (1973), Elliot et al. (1974), Elliot et al. (2017), Elliot and Collinson (2022), Fitzgerald (1994). Note that the orientation is approximately the reverse of Figure 1.

Formation. Triassic strata (Fremouw and Falla formations) are also non-marine but only locally coal-bearing. The Permian and Triassic strata (Collinson et al. 1994) accumulated predominantly in a foreland basin and are followed by the Lower Jurassic Hanson Formation, which is a mixed sedimentary-volcanic succession deposited in a rift setting (Elliot et al. 2017), and then by the Kirkpatrick Basalt, which consists of phreatomagmatic deposits overlain by flood

basalts (Elliot et al. 2021). Correlative basaltic intrusive rocks, thick sills and minor dikes, constitute the Ferrar Dolerite (Elliot and Fleming 2021). Denudation of the Gondwana sequence in post-Early Jurassic time created an extensively eroded landscape on which glaciogenic deposits accumulated in mid Cenozoic to recent time (Mayewski and Goldthwait 1985; Prentice et al. 1986; Hambrey et al. 2003; Balter-Kennedy et al. 2020).

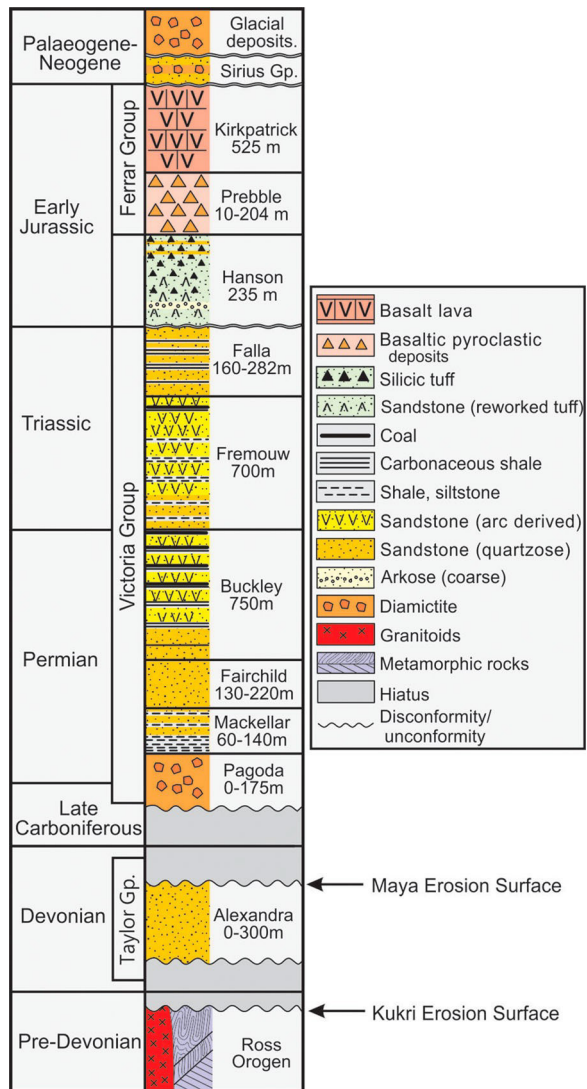


Figure 3. Simplified stratigraphic column for the central Transantarctic Mountains. Coates (1985) records a thickness of about 80 m for the Alexandra Formation at Sullivan Ridge, Ramsey Glacier. For the Shackleton Glacier region, LaPrade (1969) gives thicknesses of >60 m for the Pagoda Formation, 117 m for the Mackellar Formation, 200 m for the Fairchild Formation, and 467 m for the Buckley Formation. The Buckley Formation thickness of 750 m on this figure is appropriate for the central part of the Permian-Triassic basin. Given the limitations of estimating stratigraphic thicknesses from the interpretation of aerial photographs, USGS topographic sheets, and REMA elevations, the thickness of the Buckley Formation in the Ramsey Glacier region nevertheless appears to be substantially less than 467 m. If that proves to be the case, it suggests depositional thinning towards the margin of the Permian-Triassic basin.

Previous studies in the Shackleton Glacier region

Beacon strata at Cape Surprise (Barrett 1965) demonstrate the most significant and exposed stratigraphic offset directly related to the major dislocation along the front of the TAM. At about the same time, results of studies in the Shackleton Glacier region indicated stratigraphic offsets in Beacon rocks in the hinterland of the mountain front (LaPrade 1969; McGregor and

Wade 1969). These offsets were interpreted to document several major faults, including a horst, approximately parallel to the front.

The most significant advance since then in understanding the geological evolution has been a detailed analysis of faults (observed and interpreted) in the basement rocks east of the lower Shackleton Glacier (Miller et al. 2001) and the application of apatite thermochronology to the granitoids between Mount Munsdon and Cape Surprise (Miller et al. 2010). The former suggested an early phase of extension, orthogonal to the mountain front, followed by an episode of dextral transtension. The thermochronological studies established the timing of uplift/denudation and demonstrated that several major faults must separate those two localities. The onset was interpreted to be somewhat younger than in other parts of the TAM and most probably started at about 40 Ma and continued to about 27 Ma. The switch in stress field orientation was interpreted to have occurred at about 30 Ma. Fission track ages, as young as 19 Ma in the Beardmore Glacier region (Fitzgerald 1994), suggest uplift in the Shackleton Glacier region may have continued well into the Miocene.

On a much larger scale, structure contours on the Beacon/basement contact, from the Queen Elizabeth Range to the Shackleton Glacier region, showed that the Upper Permian and Triassic part of the Gondwana succession occupies a broad shallow trough, interpreted as a foreland basin, approximately parallel to the mountain range (Barrett et al. 1970; Barrett and Elliot 1973; Lindsay et al. 1973; Elliot et al. 1974; Collinson et al. 1994). The trough form was assumed to be the result of the uplift of the mountain front, but since the strata suggest thinning towards the basin margins, at least some was probably related to the structural evolution of the foreland basin.

Glacigenic deposits of uncertain Cenozoic age, but older than moraines clearly related to current glacial drainage, were first noted by McGregor (1965) and recognised regionally by Mayewski (1975; Mayewski and Goldthwait 1985) who assigned them to the Sirius Group. Subsequently, they were examined by Hambrey et al. (2003) who interpreted them as the result of deposition from temperate or polythermal glaciers under much warmer conditions than exist today. They established two stratigraphic units, an older Shackleton Glacier Formation and a disconformably overlying unit, the Bennett Platform Formation. They are restricted to the upper reaches of the Shackleton Glacier. A third older lithified unit was inferred from clasts found in those two formations and modern moraines. Silicified wood in this third unit suggests erosion of Beacon strata, in which Triassic silicified wood is fairly common (Barrett 1991; Taylor et al. 1991; Ryberg and Taylor 2007), rather than a Cenozoic age for the vegetation. The lithified sandy diamictite

clasts could have been derived from the Permian Pagoda Formation, suggesting this third unit was eroded directly from bedrock or reworked from post-Gondwana coarse-grained fluvial beds. The Sirius Group strata are now assigned an age of Miocene or older (pre-14 Ma; Lewis et al. 2008; Barrett 2013; Balter-Kennedy et al. 2020)

Constraints on geological maps

Assessment of the geology is constrained by a variety of factors, which include the limits imposed by the available topographic base, the difficulty of matching geological information to the REMA (Reference Elevation Model of Antarctica or REMA, Polar Geospatial Center or PGC, University of Minnesota; pgc.umn.edu; Howat et al. 2019) satellite-derived topography, and the level of geological detail given the lack of systematic mapping in this region. The available topographic maps are the USGS 1:250,000 quadrangles, which were compiled from occupied survey stations and intersected spot heights together with Trimetrogon photography (simultaneous overlapping vertical and oblique photos). The contour interval for these maps is 200 m and the areas of rock exposure are delineated. The REMA topography, for which contour intervals as little as 10 m can be superimposed, is for the greatest part excellent. However, linking the Trimetrogon photographic imagery to the REMA topography can be difficult when it comes to establishing elevations of important stratigraphical horizons. It should be noted that there appear to be small-scale discrepancies between the USGS and REMA topographic elevations, with differences of 200 m or more for a few clearly identified features (e.g. summits).

For the Gondwana succession, stratigraphic sections are available for a number of localities, and extrapolation to adjacent outcrops is possible. Fortunately, the stratigraphic column has a number of well-defined contacts which show up well on photography, specifically the basement/Beacon contact (the Kukri/Maya Erosion Surface), and the abrupt change in lithology at the Mackellar/Fairchild and Buckley/Fremouw formation contacts (both marked by an abrupt change from shale-dominated strata to sandstones). Dolerite sills are widespread, particularly in the Permian part of the section, however, sills may change thickness, change stratigraphic position, and individually are not necessarily extant across the whole region. This makes estimates, for instance, of the sub-ice elevation of the Kukri/Maya Erosion Surface unreliable.

In general, elevations of a few stratigraphic contacts can be established to about ± 25 m, and several can be assessed to ± 100 m (estimated from REMA data). Thus, local stratigraphic offsets can be inferred at a number of places. Three stratigraphic offsets, however, involve hundreds of metres of displacement.

Superimposed on these limitations is the low regional dip ($\leq 6^\circ$) inland from the TAM frontal escarpment. The low dip can be calculated approximately from REMA elevations in a few places, but the low dip meant that during stratigraphic studies, attitude information was a minor issue. Higher dips have been measured in a few places (see Structure section).

Structure

Beacon strata have a low to very low dip away from the TAM front. Actual field measurements are few: LaPrade (1969) recorded dips of $<6^\circ$ at Mount Heekin, Cumulus Hills, and Lockhart Ridge (Figures S4 & S5), and higher dips at Mount Butters (Figure S2) and on the north side of Yeats Glacier (Figure S5) (16° and 54° respectively). A similar dip of 16° to the south-southwest was measured at Mount Butters (Figure S2) on the Pagoda and Mackellar formations, a dip of 3° to the southwest was determined on Fremouw strata in the 'fault block' at Mount Rosenwald (Figure S4), and about 6° at Mount Black (Figure S4) also on Fremouw strata. The Fremouw and Falla beds at 'Alfie's Elbow' (unofficial name) southeast of Schroeder Hill (Figure S7) have a low dip to the southwest (Elliot and Collinson 2022). Interpretation of geological maps, based on field observations, airphotos and REMA data, suggest a $2\text{--}3^\circ$ southerly dip on the contact between Alexandra Formation sandstones and Pagoda Formation beds at Sullivan Ridge, on a dolerite sill south of Reid Spur, both adjacent to Ramsey Glacier (Figure S1), and a $5\text{--}6^\circ$ dip to the southwest on the Kukri/Maya Erosion Surface between northern Mount Wade and outcrops ~ 5 km to the south-southwest (Figure S3).

The inferred and observed faults together with estimated elevations of Buckley-Fremouw formation contacts are presented in Figure 4. Faults were observed in outcrop between Collinson Ridge and Gillespie Glacier (Figure S5), and at Layman Peak (Figure S1); orientations at the former are approximately north-northwest to south-southeast, and at the latter north-east-southwest. Interpretations of the stratigraphy from USGS/PGC aerial photographs suggest faults trending approximately east-west at Sullivan Ridge and Reid Spur, north-south on the east flank of Reid Spur (all on Figure S1), and north-northeast to south-southwest at Mount Boyd (Figure S2). Faults, oriented at about 125° , with displacements of a few hundred metres are present on Roberts Massif (Figure S7) (LaPrade 1969), and a somewhat greater displacement separates Everett Nunatak from Roberts Massif (Elliot and Collinson 2022). Balter-Kennedy et al. (2020) report an offset of 300–340 m for the fault just north of Misery Peak, which trends east-southeast and forms an escarpment visible across the whole of Roberts Massif. Everett Nunatak and the two fault

blocks to the south at Roberts Massif (Figure S7) have estimated low dips ($<4^\circ$) to the south-southwest based on a combination of the geological map and REMA data. The same data combination suggests a number of faults with offsets of more than 200 m occur in the Ramsey Glacier region (Figure S1). The displacement of the Kukri/Maya Erosion Surface on either side of the lower Shackleton Glacier suggests 300–400 m of offset down to west (Miller et al. 2010). Of particular significance is the estimated 750 m displacement of Fremouw strata at Mount Rosenwald (*in situ* top of the lower member of the Fremouw Formation at about 2750 m, and the base of the down-dropped middle Fremouw member at about 2000 m (Collinson and Elliot, sections JE and 86 respectively), and an 850 m offset on the Permian/Triassic boundary between Mount Black and Kitching Ridge (Figure S4). As noted by Miller et al. (2010), south of Mount Hall (Figure S3) (USGS Shackleton Glacier topographic map and on airphoto USGS/PGC TMA 2192, 33R 0079), a surface (approximately 2×5 km) is inclined towards the TAM. This may represent the Kukri/Maya Erosion Surface dipping towards the mountain front. Assuming this is correct and using REMA-derived elevations, then with an estimated 3° dip to the south-southwest, the erosion surface projects about 400 m below the elevation of the Beacon/basement contact at the escarpment front. A major north-northeast facing fault should therefore lie inboard of Mount Hall. A strong geomorphological fabric with similar orientation and most probably related to faulting is evident in the topography and the trends of glaciers outboard, but not inboard, of the Transantarctic Mountains escarpment between Mount Hall and lower Shackleton Glacier (Figure 4).

Interpretation

The age of faulting outboard of the TAM escarpment is well constrained by the offset of fission-track isochrons to late Eocene through to late Oligocene time (40–27 Ma) (Miller et al. 2010). Inboard of the escarpment offsets measured in hundreds of metres could be assigned a similar age but the orientations of most of them makes this uncertain. Some of the lesser offsets could well date from the late Cretaceous or early Cenozoic on the initial slow uplift/denudation inferred from thermochronological data for the Scott Glacier region (Fitzgerald and Stump 1997) and also inferred from secondary mineralisation in the Kirkpatrick Basalt (Fleming et al. 1999) and the Buckley Formation at Rougier Hill (Elliot et al. 2004).

The result of rapid uplift/denudation is documented between Mount Munson and Cape Surprise by major faults, which are parallel or sub-parallel to the major bounding fault marking the crustal thickness boundary separating East and West Antarctica and,

in this region, inferred to trend northwest-southeast along the coast (Miller et al. 2010). Given the general pattern of faulting associated with rift margins, in which faults in the frontal fault system may be accompanied by extension in the hinterland, three faults with appropriate orientations have been identified in the Roberts Massif region (LaPrade 1969; Elliot and Collinson 2022). These three near-parallel faults (Figure S7) define blocks that have been tilted about $3\text{--}4^\circ$ to the south-southwest. These are the only faults in the TAM hinterland that are parallel to the frontal fault system. They could be interpreted as the surface expression of listric faults that merge at depth into a detachment surface related to the development of the East Antarctic-West Antarctic lithospheric boundary and/or the frontal fault system. It should be noted that this suggested detachment surface would root to the north east as opposed to the westward rooting of detachment faults proposed by Fitzgerald and Baldwin (1997) to explain the uplift of the TAM.

Previously LaPrade (1969) and McGregor and Wade (1969) suggested the offset at Mount Rosenwald is another range-parallel fault, with a displacement of <150 m, and they indicated its extension in the northern Cumulus Hills adjacent to McGregor Glacier (Figure 4; see also Figures S4, S5). No fault, however, has been identified in the Cumulus Hills with offset comparable to the ~ 750 m of displacement of Beacon strata estimated at Mount Rosenwald (Figure 5). This estimate is based on a section of the Fremouw Formation, which includes about 30 m of the upper member (Collinson and Elliot 1984, section 86), measured in the down-dropped block and a section of the lower member of the Fremouw Formation measured on the northeast face of Mt. Rosenwald (Collinson and Elliot 1984, section JE) above the saddle. Given the lack of evidence for major displacement along the proposed trend of the fault, it is suggested here that the down-dropped block of Triassic strata at Mt Rosenwald is part of a major landslide, which is comparable to landslides identified in the Queen Alexandra Range (Elliot 2021). The down-dropped Fremouw Formation section (Collinson and Elliot 1984, section 86) lies adjacent to outcrops with dips up to 20° and southeast of prominent ridges with Fremouw beds having different attitudes (from aerial observation, LaPrade [1969] inferred a local dip of about 16°). The timing of this inferred landslide is problematic. Given its position on the modern terrain, where it is adjacent to, but not abutting, the flanks of Mount Rosenwald, and the known very slow rate of denudation under a polar climate ($<<5$ cm/m.y. Balter-Kennedy et al. 2020; 1–6 cm/m.y. Dry Valleys, southern Victoria Land, Dickinson et al. 2012), it is inferred to date from either late in the time of warm-based glaciation that terminated at about 14 Ma or early in the time of cold-based glaciation.

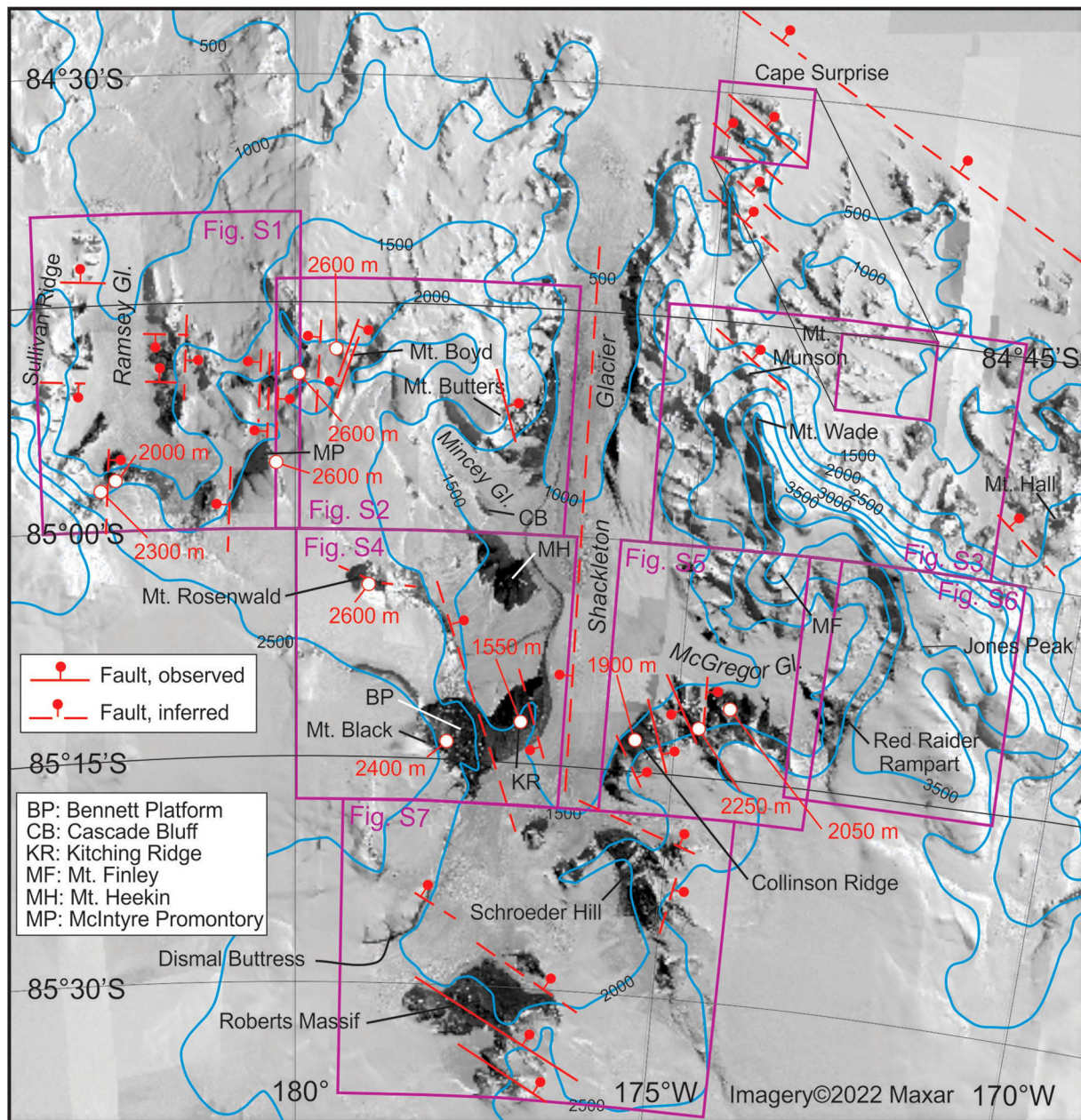


Figure 4. Faults identified in the Shackleton Glacier region. Estimated elevations (uncertainties of 50–100 m) of the Permian-Triassic boundary (Buckley-Fremouw formation contact) locations are in red. Only the major offsets between Mount Munson and Cape Surprise documented by Miller et al. (2010) are illustrated here. Contours, from Gerrish et al. (2020), are in metres, and are not precisely positioned elevations. The satellite-derived base image provided by the Polar Geospatial Center.

To account for basement granite exposed at Cascade Bluff adjacent to Mincey Glacier (Figure 4, Figure S2), LaPrade (1969) proposed a range-parallel horst between Mount Butters and Mount Heekin. The north bounding fault was projected to cut Permian strata north of Yeats Glacier but no stratigraphic offset of appropriate magnitude is evident on USGS aerial photographs. The south bounding fault was projected to pass through a fault zone identified at Lockhart Ridge (LaPrade 1969) and to cut through Permian strata near Mount Finley (Figure S2) and Permian-Triassic strata at Jones Peak (Figure S6), but again no detectable and significant faults are evident on USGS aerial photographs. Given the known relief of the Kukri and Maya erosion surfaces, which is as

much as 700 m (Isbell 1999), it is here suggested that the occurrence of granite at Cascade Bluff is the result of palaeotopography on the combined erosion surface, relief which needs to have been no more than 200–300 m. In the central TAM (Figure 2), the Pagoda Formation at Mount Munson just north of Mount Wade (Figure S3) (Ives and Isbell 2021) is only a few metres thick and overlies basement granite, is absent at Mount Bowers 100 km to the west (Figure 2) (Elliot et al. 2014), and near Clarkson Peak 200 km to the northwest (Figure 2) is only a veneer on Devonian sandstones (Elliot and Isbell 2021).

A 6° southwest dip of the Beacon strata at the northwestern end of the Mount Heekin massif (LaPrade 1969) implies a down to the northeast fault

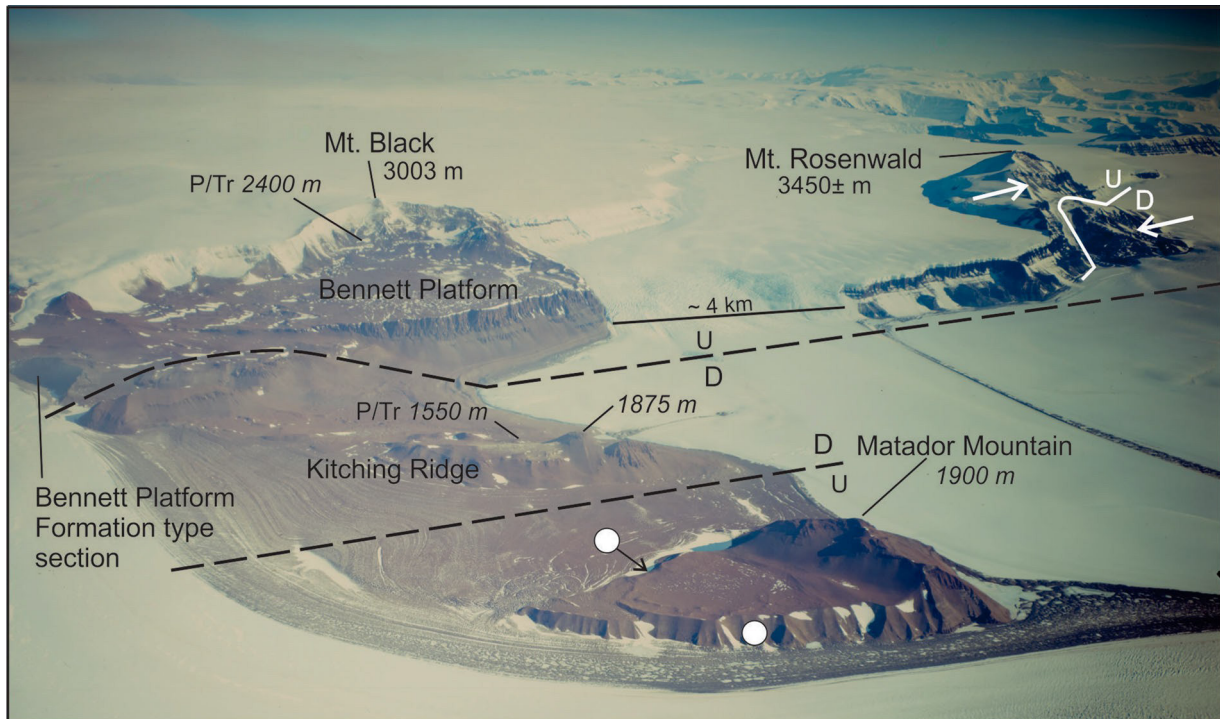


Figure 5. Aerial photograph, view to the west, to illustrate the proposed faults at Mount Rosenwald and in the Mount Black-Matador Mountain region. White arrows point to the estimated locations of the contact between the lower and middle members of the Fremouw Formation at Mount Rosenwald, indicating ~ 750 m of offset. The Permian/Triassic boundary is indicated by P/Tr. Approximate locations (white circles) of Sirius Group deposits (Bennett Platform Formation) southeast of Matador Mountain from Hambrey et al. (2003); it is possible that Sirius strata are widespread beneath the veneer of surficial debris, rather than banked against bedrock. The outcrops behind the white circles are 50–100 m high, based on REMA data. Given this is an oblique photograph, the horizontal scale applies only at its location on the figure. The geology is illustrated on Figure S4. Elevations in italics estimated from REMA data; others from USGS Liv Glacier topographic sheet. Photograph enlarged from PGC/USGS photo TMA 2189 R33 030.

between Mount Heekin and Mount Rosenwald, which would have had approximately 1000 m of offset (3° dip would give a 500 m offset) if located adjacent to Mount Rosenwald. Although this would be consistent with LaPrade's (1969) view that the displacement at Mount Rosenwald is due to faulting, a landslide origin, as advocated earlier, is the preferred interpretation. This interpretation does not exclude faults between mounts Heekin and Rosenwald.

The Permian/Triassic boundary is exposed at Mount Black at a REMA-estimated elevation of about 2400 m and at Kitching Ridge at a REMA-estimated elevation of 1550 m, an 850 m elevation difference (Figures 4 and 5, Figure S4) (Collinson and Elliot 1984, sections JA and 90). Buckley Formation beds intruded by dolerite sills form the lower slopes of Mount Black and all the bedrock geology of Bennett Platform. At Kitching Ridge, the section consists of a thin interval of Buckley beds overlain by the lower member of the Fremouw Formation. The section is surrounded by dolerite, but even allowing for consequent uncertainties, it must have been dropped relative to Bennett Platform. Buckley Formation beds are present up to about 1850 m elevation at Matador Mountain and therefore a fault, down to the southwest, must isolate Kitching Ridge in a small graben.

A major fault, down to the northeast, must lie between Bennett Platform and Kitching Ridge. The fault cannot be oriented parallel to the frontal fault because the stratigraphy both to the west-northwest (in particular) and east-southeast along a range-parallel trend shows no comparable displacement, if any. An escarpment aligned northwest-southeast, which heads northwestwards towards Mount Rosenwald, is oriented parallel to the northeast-facing front of Bennett Platform and is interpreted to mark the trend of the fault. The fault trend to the southeast would pass just to the northeast of Roberts Massif, and to the northwest it would cut through the Bush Mountains near Mount Boyd where a number of faults have been identified, but none with such a large offset (Figure S2).

The Permian-Triassic boundary at Collinson Ridge (Figure S5), directly east of Kitching Ridge, is located at a REMA-elevation of 1900 m, which gives a similar offset (ca. 350 m, down to the west beneath the Shackleton Glacier) to that determined for displacement (300–400 m) of the Kukri/Maya Erosion Surface across Shackleton Glacier between Mount Wade and Mount Butters. To the south, along the trend of this inferred fault, a reliable estimate of offset is not possible because of the lack of detailed stratigraphic data

and/or a key horizon. Fremouw strata are present at Dismal Buttress (Figure S7) up to an elevation of about 2200 m, but there are no overlying massive sandstone cliffs similar to the basal Falla beds at Mystery Peak 8 km to the southeast across Shackleton Glacier at an elevation of about 2350 m. However, at Half Century Nunatak about 10 km to the north at a REMA estimated elevation of about 2300 m (c.f. about 2600 m on the Liv Glacier topographic map) a succession of pale-coloured resistant sandstone ledges, which resemble Falla strata cropping out south of Schroeder Hill (Elliot and Collinson 2022), is interpreted to belong to that formation. Falla strata are not present at Mount Black, which has an elevation of 3000 m, and if correctly identified at Half Century Nunatak, the Fremouw-Falla contact will have a low southerly dip ($\geq 3^\circ$). This implies a down to the north fault between Half Century Nunatak and Dismal Buttress, which is supported by a sliver of Falla strata, at a REMA estimated elevation of 2200 m, identified along the Shackleton Glacier valley wall north of Dismal Buttress (Figure S7).

In addition to the offsets recorded by the Buckley/Fremouw contact just described, significant displacements are also inferred in the Ramsey Glacier region (Figure 4, Figure S1). At the southern end of Sullivan Ridge, based on airphoto interpretation of the distribution of the Fairchild Formation, a fault with a throw of about 700 m, down to the south, must be present. At the northern end of Reid Spur, a fault with a throw of about 500 m must separate basement metamorphic rocks to the north from Permian strata to the south. Five other faults with lesser offsets are also inferred in that region.

Matador Mountain, with a summit elevation (REMA) of about 1900 m and comprising Permian Buckley beds and Ferrar dolerite sills, is approximately the same elevation as the Buckley-Fremouw contact at Collinson Ridge, which would suggest little offset along the Shackleton Glacier fault and that the fault dies out southwards. In this case, the Kitching Ridge block is offset from Collinson Ridge by the graben faults, not the fault along the Shackleton Glacier.

Small faults were observed in the field at Layman Peak (Figure S1) and Collinson Ridge (Figure S5), as already noted. From examination of aerial photographs, small displacement faults were also identified at Mount Boyd and in the Ramsey Glacier region. Those at Mount Boyd trend in the northeast-southwest quadrant, but in the Ramsey Glacier region can only be interpreted as approximately north-south or east-west. Without detailed structural studies, no relationship to the frontal fault system can be inferred such as has been described for the Cape Surprise area (Miller et al. 2001). Faults with small displacements (<10 m) are widespread, as also noted by Hambrey et al. (2003), and some displace Sirius strata.

In a more regional context, 200 km to the southeast in the Scott Glacier region (Figure 1), Katz (1982), on the basis of field data and close examination of aerial photographs, documented a small set of faults parallel to the frontal fault system, and a subsidiary set of conjugate faults oriented at about 45° to the front. Later, Fitzgerald and Stump (1997) also identified faults oriented at an angle to the frontal fault system but based on fission track data. A similar distance westwards in the upper Beardmore Glacier region (Figure 2) a small graben and a northeast facing monocline are approximately parallel to the frontal fault system. A normal fault down to the east offsets Triassic strata along the eastern part of the Dominion Range and is interpreted to displace glaciogenic strata on the Meyer Desert; any late Cenozoic displacement is only a few metres whereas from Triassic stratigraphy and aerial photograph interpretation the fault has about 200 metres of offset (McGregor 1965; Elliot et al. 1974) (note that McGregor's Dominion Coal Measures at his Locality D and forming the upper part of his Locality C are now assigned to the upper member of the Fremouw Formation). It is oriented at about 10° to the frontal fault system, and approximately perpendicular to this a fault displaces Permian and Triassic strata at the northern end of Supporters Range (Elliot et al. 1974). The monocline at Mount Falla (Figure 2) is oriented perpendicular to the frontal fault system (Barrett and Elliot 1973). East of Mount Achernar (Figure 2), a narrow horst, exposing west-dipping (ca. 45°) lower Permian strata, a west-facing monocline, and a small displacement fault are all oriented at about 40° to the frontal fault system (Elliot et al. 2017). A west-facing monocline is located on the western flank of the Queen Elizabeth Range (Figure 2) (Barrett et al. 1970), which suggests a graben may underlie Marsh Glacier. This putative graben is oriented at a slightly smaller angle (about 30°) to the frontal fault system. The other flank of this graben is marked by the Marsh Fault, which has several hundred metres of displacement and brings Proterozoic rocks to the surface. A fault of lesser displacement but also facing east cuts the graben east of Moody Nunatak (Figure 2).

Except at Cape Surprise, few faults are parallel or close to parallel to the frontal fault system. Collapse along the frontal fault system appears not to have been accompanied by any significant extension in the hinterland, except possibly at Roberts Massif and the upper Beardmore Glacier region. The conjugate fault set approximately orthogonal to the frontal fault system at Cape Surprise (Miller et al. 2001) is replaced by a conjugate set oriented at a moderate angle ($40-45^\circ$) in the lower Scott Glacier region (Katz 1982; Fitzgerald and Stump 1997). Conjugate fault sets are not clearly repeated, if at all, elsewhere in the central TAM. It should be noted that structural

features associated with Ferrar Dolerite dike emplacement and Gondwana break-up (Wilson 1992, 1993) may have imposed regional weaknesses that were exploited during late Mesozoic and Cenozoic tectonism. In the Queen Alexandra Range region (Wilson 1993), those Ferrar-age conjugate faults are oriented approximately parallel (north-northwest to south-southeast) and perpendicular (northeast-southwest) to the frontal fault system.

The simplest assessment of the age of significant faulting in the Shackleton Glacier region would be that all are mid-Cenozoic (ca. 40 < 27 Ma) and entirely associated with the time of rapid development of the Transantarctic Mountains front, however that is problematic. The range-parallel faults in the Roberts Massif region most probably occurred during that time. Slow uplift/denudation may well have occurred during the Cretaceous and earlier in Cenozoic time and probably would have been accompanied by less significant faulting unrelated to the later frontal fault system. Most faults fall into that category, and it is suggested that the Ramsey Glacier region faults may pre-date rapid uplift. Major faulting probably ceased by about 20 Ma, when uplift slowed greatly, although minor faulting with lesser offsets may have continued at least to the end of the Miocene. Slow uplift post-14.5 Ma is most likely the result of isostatic rebound (Balster-Kennedy et al. 2020 and references therein) and/or glacial erosion (Stern et al. 2005; Golledge et al. 2014). If correct, it suggests faults with throws of 100 m or more are more likely to date from the earlier stages of uplift.

Sirius Group

The Sirius Group is widespread in the Transantarctic Mountains (Denton et al. 1991) but its age is not well established, not the least because strata assigned to the Group occur in a variety of topographic settings some of which are mutually incompatible for a single event. Sirius-like sediment occurs in southern Victoria Land on the shoulder of Mount Feather (Figure 1) about 800 m above adjacent glaciers (Wilson 2002); caps an isolated nunatak (Mount Sirius), south of the Bowden Névé (Figure 2) (Mercer 1972; Harwood 1986); occurs at elevations of 3300 m adjacent to Mount Falla (Figure 2) (Prentice et al. 1986); is lodged in a cleft on the summit ridge of Mount Block (Grosvenor Mountains, Figure 2) at about 2770 m; is plastered on Fremouw strata on the south-facing wall of the Shackleton Glacier flank at Dismal Buttress (McGregor 1965) where it also overlies a dolerite sill (Hambrey et al. 2003); overlies modern topography on the east side of Otway Massif and is draped on a modern landform southeast of Schroeder Hill (Elliot and Collinson 2022); is plastered on a large glacially grooved pavement at Roberts Massif (Hambrey et al.

2003); and forms a 100 + m wall facing the Shackleton Glacier on the east flank of Bennett Platform and also fills clefts in the platform surface (Hambrey et al. 2003). The range of topographic settings suggests deposition of Sirius-like sediment must span a significant time period and is unlikely to be the result of a single event, as established by Hambrey et al. (2003) who recognised two principal lithostratigraphic units for the Shackleton Glacier region. The most reliable age estimate for the Sirius Group comes from southern Victoria Land where radiometric dating of volcanic ash established a minimum age of about 14 Ma (Lewis et al. 2008; Barrett 2013) with the maximum being the onset of warm-based glaciation at about 34 Ma. This age assignment is strengthened by exposure-age dating of moraines related to cold polar ice on Roberts Massif, which are all younger than 15–14 Ma (Balster-Kennedy et al. 2020). The Sirius Group was deposited during the early phase of warm-based Antarctic glaciation, which at about 14 Ma switched to cold-based glaciation. In this context, the ‘Alfie’s Elbow’ Sirius deposit southeast of Schroeder Hill, consisting of bedded sandy sediment which is draped on modern topography (Elliot and Collinson 2022), is clearly an anomaly and deserves further investigation.

Hambrey et al. (2003) attributed the different elevations of the older Shackleton Glacier Formation deposits to post-deposition faulting; only in the Roberts Massif region is the formation demonstrably offset and no major fault has been identified between there and Bennett Platform. The strata, interpreted as mainly lodgement till, suggested a low relief terrain existed at the time of deposition beneath a polythermal ice sheet. Thermochronological data show that rapid uplift and denudation was initiated at about 40 Ma, however, the frontal fault system and associated uplift could not have caused significant faulting in the hinterland until after deposition of the Shackleton Glacier Formation. Recognising that uplift in the hinterland diminished away from the Transantarctic Mountains escarpment and accepting a single depositional episode, the formation must date to an early stage of glaciation before any significant topography or stratigraphic offsets had been imposed on the Permian and Triassic succession by rapid Cenozoic uplift. Thus, Cretaceous and/or early Cenozoic faulting in the hinterland could have yielded minor stratigraphic offsets and contributed to slightly differing depositional elevations of the Shackleton Glacier Formation. The lodgement till deposits of the Shackleton Glacier Formation document a particular depositional environment; on lithostratigraphic grounds they can be correlated but chronostratigraphic correlation is not possible without reliable age determinations. Therefore, the varied depositional elevations could in part be the result of multiple advances and retreats

occurring simultaneously with ongoing tectonism and faulting. Based on the interpretation that the younger Bennett Platform Formation was deposited along or adjacent to an ancestral Shackleton Glacier (Hambrey et al. 2003), then the Sirius strata about 6 km southeast of Misery Peak and in valleys facing south probably belong to the Shackleton Glacier Formation, in which case at least 400 metres of local relief existed at the time of their deposition.

The results of the Cape Roberts and ANDRILL projects show that there were multiple ice advances and retreats during Oligocene and Early Miocene time in south Victoria Land (Cape Roberts Science Team 2000; Fielding et al. 2011; Passchier 2012; McKay et al. 2016). Of more direct relevance are the two Lower Miocene volcanic edifices now at about 2000 m elevation and ~300 km distant at the head of the Scott Glacier (Figure 1) (Stump et al. 1980, 1990a, 1990b). Re-examination of the two exposed volcanoes has shown that one (dated at ~20 Ma) was erupted subglacially whereas the other with an age of ~16 Ma is interpreted to have been erupted into a pluvial lake (Smellie and Panter 2021). Bedrock surface elevations during volcanism are constrained only so far as rapid uplift and denudation in the lower Scott Glacier region ceased by about 40 Ma although denudation must have continued until at least the switch to cold-based glaciation (Fitzgerald and Stump 1997). Isostatic uplift post-40 Ma is probable but significant uplift (a thousand metres or more) after about 16 Ma seems improbable. In the upper Shackleton Glacier region isostatic uplift post-14.5 Ma is estimated to be ~350 m (Balter-Kennedy et al. 2020). If the Miocene pluvial lake environment in the upper Scott Glacier region is correct, it implies a dramatically warmer climate shortly before the switch to cold-based glaciation and that the terrain would have been at an elevation only a few hundred metres less than that of today.

The Gondwana succession throughout the TAM must have been subjected to sub-aerial erosion from the Middle Jurassic to the onset of slow uplift in the Cretaceous. In the lower Scott Glacier region (Figure 1), denudation in the Early and Late Cretaceous uplift episodes amounted to less than 2 km each (Fitzgerald and Stump 1997) and presumably comparable denudation may have occurred in the lower Shackleton Glacier region. Erosion continued until the onset of more rapid uplift in early Cenozoic time throughout the TAM, and therefore the postulated low relief terrain at the inception of glaciation (about 34 Ma), as suggested by the Shackleton Glacier Formation, may have been a TAM-wide landform. At Roberts Massif a glacially grooved surface is exposed in the northern lowlands (Hambrey et al. 2003) and also on the lip of the upthrown side of a range-parallel fault immediately south of ‘The Bowl’ (unofficial name) (Figure S7). That fault, according to the interpretation of

Balter-Kennedy et al. (2020), predates moraines, which have exposure-age dates ranging from 15–14 to 3–1 Ma. Therefore at least that glacial surface was demonstrably displaced by faulting. If the low-relief terrain existed into the Middle Miocene, it would imply that faulting at Roberts Massif occurred very late in the existence of that terrain. It also implies limited erosion and landscape development until late in the existence of warm-based glaciation, which seems improbable. Therefore, it is suggested that the Shackleton Glacier Formation belongs to an early stage of glaciation during early Oligocene time, whereas the Bennett Platform Formation was deposited during or after an ancestral Shackleton Glacier valley system had been carved in late Oligocene to mid Miocene time. Because the Bennett Platform Formation at Dismal Buttress (Hambrey et al. 2003) is located about 200 m a more than the Shackleton Glacier, deposition there probably occurred relatively early in the carving of the valley system and may therefore have a late Oligocene age. The other outcrops of the formation are less than a hundred metres above current ice level and therefore probably were deposited in Early Miocene time.

The distribution of the Bennett Platform Formation adjacent to and southeast of Matador Mountain is uncertain; it might be an extensive sheet rather than plastered on the flanks of a bedrock platform. Regardless, at Matador Mountain (Hambrey et al. 2003) it lies at a REMA elevation of 1400–1500 m whereas at the type section (on the east flank of Bennett Platform about 12 km to the south) it occurs at a REMA elevation of 1750–1850 m (Figure 5, Figure S4) (REMA elevations are, respectively, 200 and 100 m lower than those reported by Hambrey et al. 2003). This difference in outcrop elevation may simply reflect deposition at different elevations along the ancestral Shackleton Glacier, although if the formation is a lateral deposit of the glacier, younger ice locally removed the valley wall and greatly modified the previous palaeotopography. Alternatively, the elevation difference may indicate a fault with an estimated throw of 250 m down to the northeast between Matador Mountain and Bennett Platform, reactivating one or both of the bounding faults of the Kitching Ridge graben identified on the offsets of the Permian and Triassic bedrock (Figure 5). Reactivation of the fault between Bennett Platform and Kitching Ridge would have increased the displacement from about 600 to 850 m. Displacement on the other bounding fault, between Kitching Ridge and Matador Mountain, would imply a switch from down to the southwest to down to the northeast on a new fault. In either case, faulting would have occurred late in the history of warm-based glaciation and late in the history of tectonism.

The type section of the Bennett Platform Formation lies along the flanks of the Shackleton Glacier,

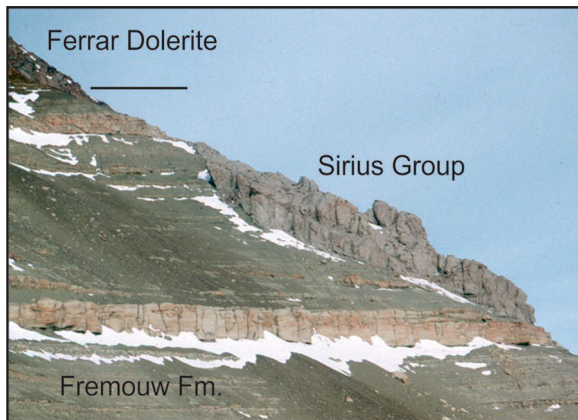


Figure 6. Sirius Group deposits plastered on Fremouw Formation strata at Dismal Buttress. Scattered large dolerite clasts are visible in the Sirius beds. The lower part of the outcrop is tentatively correlated with the outcrop illustrated by McGregor (1965, Figure 3), which he estimated is about 40 feet (12 m) high; accepting the correlation, the exposure illustrated here is about 120 feet (36 m) high. View towards the east. Photograph by the author.

suggesting a protracted time interval followed deposition of the Shackleton Glacier Formation. During this interval a landscape with incised glacial valleys, not too dissimilar to today's topography, was developed (Hambrey et al. 2003). Old glacial deposits, first reported and illustrated by McGregor (1965), are perched high on the south-facing valley wall of the Shackleton Glacier at Dismal Buttress (Figure 6). The deposits, sitting about 200 m above Shackleton Glacier and plastered on a steep slope of Fremouw strata, comprise weakly bedded diamictite, containing dolerite and sandstone clasts, overlain by unstratified till (McGregor 1965, Figures 3 and 4). These Sirius strata represent glacial sedimentation on essentially modern topography but at an early stage in the carving of the glacial valley. From the perspective of the topographic setting and the presence of dolerite clasts, the strata should be assigned to the Bennett Platform Formation. However, it seems improbable that they were contemporaneous either with the type section of the Bennett Platform Formation, which is located about 25 km to the north and up to about 100 m above ice level, or with the Bennett Platform Formation beds documented by Hambrey et al. (2003) at a higher elevation overlying dolerite on the northern flank of Dismal Buttress.

Palaeotopography

Brandau Glacier, west of the Ramsey Glacier, is remarkable for the beheading of its upper reaches by headwall advance of the Muck Glacier (Figure 7). Brandau Glacier is about 6 km wide at its upstream truncation where the elevation difference between

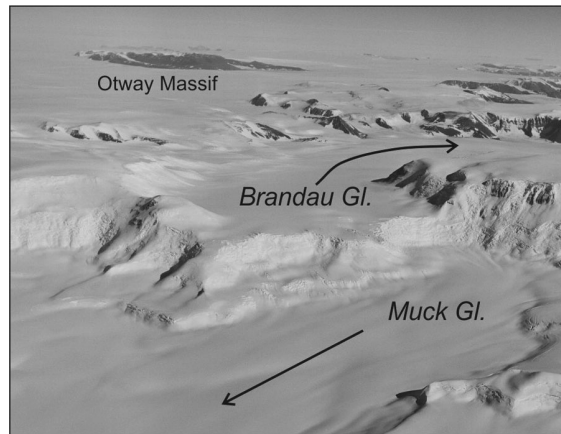


Figure 7. The upper reaches of Brandau Glacier are truncated due to headward erosion by Muck Glacier (locations on Figure 2). Brandau Glacier is about 6 km wide at its truncation. Arrows indicate direction of glacier flow. View towards the south-south west. Photograph enlarged from PGC/USGS photo TMA 781 R33 029.

the two glaciers is about 500 m. The lip at that point is most likely to be a dolerite sill.

Four glaciers in this part of the TAM flow inland from the escarpment (Figure 2; Keltie, Brandau, Mincey, upper McGregor glacier) and record earlier pre-glacial fluvial drainage on the backside of the rising escarpment. Erosion and valley enlargement would have been enhanced on the onset of rapid uplift. At the same time, erosion and associated fluvial systems would have driven the developing escarpment inland. The surface east and southeast of Mount Hall, which is a possible outlier of the Kukri/Maya Erosion Surface, would be an expression of the escarpment retreat. The probability of drainage into the continental interior in the central TAM was first noted by Huerta (2007) who interpreted it in terms of a Mesozoic plateau in West Antarctica (Bialas et al. 2007) rather than Cenozoic rift-shoulder uplift of the TAM, which, here, is the preferred scenario. It is possible that the cirque-like topographic features along the southern flank of Roberts Massif document south-flowing ice from local highs during the early stages of glaciation.

Conclusions

Faults and inferred faults are relatively common in the Shackleton Glacier region and range widely in displacements and orientations. A small number have been identified directly in the field, but most are inferred from displacement of strata, made evident by mapping of widely separated outcrops.

Three displacements of 700 or more metres are recognised. The stratigraphic displacement (~ 750 m) of Triassic strata at Mount Rosenwald is interpreted to be the result of a landslide, which occurred after much of the present-day topography had been formed

and therefore must date from the Middle Miocene. The 850 m offset between Bennett Platform and Kitching Ridge is interpreted as a Cenozoic tectonic fault, oriented at a high angle to the frontal fault system, and dating from Oligocene-Early Miocene time during rapid uplift/denudation of the TAM. The third ~700 m displacement occurs in the Ramsey Glacier region where fault displacements of 200–300 m are common. None of these offsets is demonstrably parallel to the frontal fault system. The age of these Ramsey Glacier faults is uncertain, but may record an early stage (possibly pre-40 Ma) of uplift of the TAM in this region rather than documenting the rapid uplift. Range-parallel faults, with displacements of hundreds of metres and probably related to the frontal fault system, are confined to the Roberts Massif region. Smaller displacement faults are recognised by direct field observation and could have occurred at any time in the history of tectonism, including Late Miocene time or younger.

Accurate elevations and attitude measurements of Gondwana strata throughout the region are required if assessment of the observed and inferred faults is to be improved. Close examination of the directly observed faults might yield information that would better establish their timing, such as determining if datable phyllosilicate minerals occur along fault planes.

Sirius Group strata are older than mid-Miocene (>14 Ma) (Lewis et al. 2008). The Shackleton Glacier Formation, given the dominance of lodgement till and its low relief depositional environment (Hambrey et al. 2003), is interpreted to date from the early stages of warm-based glaciation (and uplift) and therefore to have an age of early Oligocene (34–30 Ma). It may represent several different depositional events. The Bennett Platform Formation is suggested to have a late Oligocene age at Dismal Buttress, whereas at Bennett Platform and Matador Mountain an Early Miocene age.

The Shackleton Glacier region may be the best place outside the Dry Valleys of southern Victoria Land for the investigation of the Sirius Group deposits and their relationships to modern topography and the development of the Transantarctic Mountains.

Acknowledgements

Field work on which this paper is based was conducted principally in the 1970–1971 and 1995–1996 seasons, with additional minor field observations during the 2007–2008 season. DEMs produced using data from Maxar. David Sadler gave invaluable help with Figure 4. Reviews by Paul Fitzgerald and an anonymous reviewer improved the manuscript significantly. Byrd Polar and Climate Research Center contribution no. 1619. Satellite imagery (Figure 4) provided by the Polar Geospatial Center under NSF-OPP awards 1043681 and 1559691. DEM provided by the Byrd Polar and Climate Research Center and the Polar Geospatial Center under NSF-OPP awards 1543501, 1810976, 1542736, 1559691, 1043681, 1541332, 0753663, 1548562, 1238993

and NASA award NNX10AN61G, and the Blue Waters Innovation Initiative.

Disclosure statement

No potential conflict of interest was reported by the author(s).

Funding

All were supported by the Office of Polar Programs, National Science Foundation, Washington DC (NSF grants GA-26652, OPP-9420498, and OPP-0636824).

Data availability statement

Supplemental files (Text plus Figures S1–S7) are geological maps at a scale of 1:250,000 of the Shackleton Glacier region, Transantarctic Mountains. Maps are JPEG images. These data are openly available in Figshare at <https://doi.org/10.6084/m9.figshare.20490108>.

References

Balter-Kennedy A, Bromley G, Balco G, Thomas H, Jackson MS. 2020. A 14.5-million-year record of East Antarctic Ice Sheet fluctuations from the central Transantarctic Mountains, constrained with cosmogenic ^{3}He , ^{10}Be , ^{21}Ne , and ^{26}Al . *The Cryosphere*. 14:2647–2672. doi:10.5194/tc-14-2647-2020.

Barrett PJ, Elliot DH. 1973. Reconnaissance Geologic map of the Buckley Island Quadrangle, Transantarctic Mountains, Antarctica. United States Geological Survey, Antarctica Map A-3. 1:250,000.

Barrett PJ, Lindsay JF, Gunner J. 1970. Reconnaissance geologic map of the Mount Rabot Quadrangle, Transantarctic Mountains, Antarctica. United States Geological Survey, Antarctica 1:250,000. Antarctic Map No. 1.

Barrett PJ. 1965. Geology of the area between the Axel Heiberg and Shackleton glaciers, Queen Maud range, Antarctica. Part 2–Beacon Group. *New Zealand Journal of Geology and Geophysics*. 8:344–370.

Barrett PJ. 1991. The Devonian to Triassic Beacon supergroup of the Transantarctic Mountains and correlatives in other parts of Antarctica. In: Tingey RJ, editor. *The geology of Antarctica*. Oxford: Clarendon Press; Monographs on Geology and Geophysics. 17:120–152.

Barrett PJ. 1996. Antarctic palaeoenvironment through Cenozoic times – a review. *Terra Antarctica*. 3(2):103–119.

Barrett PJ. 2013. Resolving views on Antarctic Neogene glacial history—the Sirius debate. *Earth and Environmental Science Transactions of the Royal Society of Edinburgh*. 104:31–53. doi:10.1017/S175569101300008X.

Bialas RW, Buck WR, Studinger M, Fitzgerald PG. 2007. Plateau collapse model for the transantarctic mountains-west Antarctic rift system: insights from numerical experiments. *Geology*. 35:687–690.

Bradshaw M. 2013. The Taylor group (beacon supergroup): the Devonian sediments of Antarctica. In: Hambrey MJ, Barker PF, Barrett PJ, Bowman V, Davies B, Smellie JL, Tranter M, editors. *Antarctic palaeoenvironments and earth-surface processes*. London: Geological Society of

London, Special Publication; 381:67–97. doi:[10.1144/SP381.23](https://doi.org/10.1144/SP381.23).

Cape Roberts Science Team. 2000. Studies from the Cape Roberts Project, Ross Sea, Antarctica. Initial Report on CRP-3. *Terra Antarctica*. 7:1–209 with supplement.

Coates DA. 1985. Late Paleozoic glacial patterns in the central Transantarctic Mountains. In: Turner MD, Splettstoesser JF, editors. *Geology of the central Transantarctic Mountains*. Washington DC: American Geophysical Union; Antarctic Research Series. 36:325–338.

Collinson JW, Elliot DH, Isbell JL, Miller MF, Miller JMG. 1994. Permian-Triassic transantarctic basin. In: Veevers JJ, Powell CMCA, editors. *Permian-Triassic transantarctic basin, Permian-Triassic Pangean basins and foldbelts along the Panthalassan margin of Gondwanaland*. Boulder, CO: Geological Society of America; Memoir 184:173–222.

Collinson JW, Elliot DH. 1984. Triassic stratigraphy of the Shackleton Glacier area. In: Turner MD, Splettstoesser JF, editors. *Geology of the central Transantarctic Mountains*. Washington DC: American Geophysical Union; Antarctic Research Series. 36:103–117.

Cox SC, Smith Lytle B, the GeoMAP Team. 2022. SCAR GeoMAP dataset. GNS Science, Lower Hutt, New Zealand. Release v. 202208. doi:[10.21420/7SH7-6K05](https://doi.org/10.21420/7SH7-6K05).

Dalziel IWD. 1997. Neoproterozoic-Paleozoic geography and tectonics: review, hypothesis, environmental speculation. *Geological Society of America Bulletin*. 108:16–42.

Dalziel IWD, Lawver LA. 2001. The lithospheric setting of the West Antarctic Ice Sheet. In: Alley RB, Bindschadler RA, editors. *The west Antarctic ice sheet: behavior and environment*. Washington DC: American Geophysical Union, Antarctic Research Series, 77:29–44.

David TWE, Priestley RE. 1914. Glaciology, physiography, stratigraphy and tectonic geology of south Victoria Land, with short notes on palaeontology by T. Griffith Taylor. British Antarctic Expedition 1907–09, Report of Scientific Investigations, Geology, V. 1. 319 pp.

Denton GH, Prentice ML, Burckle LH. 1991. Cainozoic history of the Antarctic ice sheet. In: Tingey RJ, editor. *The geology of Antarctica*. Oxford: Oxford University Press; p. 365–433.

Dickinson WW, Schiller M, Ditchburn BG, Graham IJ, Zondervan A. 2012. Meteoric Be-10 from Sirius Group suggests high elevation McMurdo Dry valleys permanently frozen since 6 Ma. *Earth and Planetary Science Letters*. 355–356:13–19.

Elliot DH, Barrett PJ, Mayewski PA. 1974. Reconnaissance geologic map of the Plunket Point Quadrangle, Transantarctic Mountains, Antarctica. United States Geological Survey, Antarctica 1:250,000. Map A-4.

Elliot DH, Collinson JW. 2022. Schroeder hill, central Transantarctic Mountains, Antarctica: Triassic stratigraphy and Sirius Group glaciogenic deposits. *Antarctic Science*. doi:[10.1017/S0954102022000013](https://doi.org/10.1017/S0954102022000013).

Elliot DH, Fanning CM, Hulett SRW. 2014. Age provinces in the Antarctic craton: evidence from detrital zircons in Permian strata from the Beardmore glacier region, Antarctica. *Gondwana Research*. 28:152–164. doi:[10.1016/j.gr.2014.03.013](https://doi.org/10.1016/j.gr.2014.03.013).

Elliot DH, Fleming TH. 2021. Ferrar Dolerite and Kirkpatrick basalt formations II. Geochemistry. In: Smellie JL, editor. *Volcanism in Antarctica: 200 million years of subduction, rifting and continental break-up*. Geological Society of London; Memoir 55: 93–119. doi:[10.1144/M55.2018.44](https://doi.org/10.1144/M55.2018.44).

Elliot DH, Foland KA, Fleming TH. 2004. Dating paleohydrologic events with authigenic apophyllite: an example from the Permian of the central transantarctic mountains, Antarctica. *Geological Society of America, Abstracts with Programs*. 36(5):473.

Elliot DH, Isbell JL. 2021. A mass transport deposit in the Permian Mackellar formation, Victoria group, Antarctica. *New Zealand Journal of Geology and Geophysics*. doi:[10.1080/00288306.2020.1868538](https://doi.org/10.1080/00288306.2020.1868538).

Elliot DH, Larsen D, Fanning CM, Fleming TH, Vervoort JD. 2017. The lower Jurassic Hanson formation of the transantarctic mountains: implications for the Antarctic sector of the Gondwana plate margin. *Geological Magazine*. 154:777–803. doi:[10.1017/S0016756816000388](https://doi.org/10.1017/S0016756816000388).

Elliot DH, White JDL, Fleming TH. 2021. Ferrar Dolerite and Kirkpatrick basalt formations I. volcanology. In: Smellie JL, editor. *Volcanism in Antarctica: 200 million years of subduction, rifting and continental break-up*. Geological Society of London; Memoir 55:75–91. doi:[10.1144/M55.2018.39](https://doi.org/10.1144/M55.2018.39).

Elliot DH. 2013. The geological and tectonic evolution of the transantarctic mountains: a review. In: Hambrey MJ, Barker PF, Barrett PJ, Bowman V, Davies B, Smellie JL, Tranter M., editors. *Antarctic palaeoenvironments and earth-surface processes*. Geological Society of London; Special Publication. 381:7–35. doi:[10.1144/SP381.14](https://doi.org/10.1144/SP381.14).

Elliot DH. 2021. Landslides in the transantarctic mountains: Lower Jurassic and older strata displaced in late Mesozoic to late Cenozoic time. *New Zealand Journal of Geology and Geophysics*. doi:[10.1080/00288306.1929349](https://doi.org/10.1080/00288306.1929349).

Emry EL, Nyblade AA, Horton A, Hanson SE, Julià J, Aster RC, Huerta AD, Winberry JP, Wiens DA, Wilson TJ. 2020. Prominent thermal anomalies in the mantle transition zone beneath the transantarctic mountains. *Geology*. 48:748–752. doi:[10.1130/G47346.1](https://doi.org/10.1130/G47346.1).

Fielding CR, Browne GH, Field B, Florindo F, Harwood DM, Krissek LA, Levy RH, Panter KS, Passchier S, Pekar SF. 2011. Sequence stratigraphy of the ANDRILL and AND-2A drillcore, Antarctica: A long-term ice-proximal record of early to Mid-Miocene climate, sea-level and glacial dynamism. *Palaeogeography, Palaeoclimatology, Palaeoecology*. 305:337–351. doi:[10.1016/j.palaeo.2011.03.026](https://doi.org/10.1016/j.palaeo.2011.03.026).

Fitzgerald PG, Baldwin S. 1997. Detachment fault model for the evolution of the Ross Embayment. In: Ricci CA, editor. *The Antarctic region: geological evolution and processes*. Siena: Terra Antarctica Publication; p. 555–564.

Fitzgerald PG, Baldwin SL, Webb LE, O’Sullivan PB. 2006. Interpretation of (U-Th)/He single grain ages from slowly cooled crustal terranes: a case study from the transantarctic mountains of southern Victoria land. *Chemical Geology*. 225:91–120.

Fitzgerald PG, Stump E. 1997. Cretaceous and Cenozoic episodic denudation of the transantarctic mountains, Antarctica: New constraints from apatite fission track thermochronology in the Scott Glacier region. *Journal of Geophysical Research*. 102:7747–7765. doi:[10.1029/96JB03898](https://doi.org/10.1029/96JB03898).

Fitzgerald PG. 1992. The transantarctic mountains of southern Victoria land: the application of fission-track analysis to a rift shoulder uplift. *Tectonics*. 11:634–662. doi:[10.1029/9TC02495](https://doi.org/10.1029/9TC02495).

Fitzgerald PG. 1994. Thermochronologic constraints on post-Paleozoic tectonic evolution of the central transantarctic mountains, Antarctica. *Tectonics*. 13:634–662.

Fitzgerald PG. 2002. Tectonics and landscape evolution of the Antarctic Plate since the breakup of Gondwana, with an emphasis on the West Antarctic rift system and the Transantarctic Mountains. In: Gamble JA, Skinner DNB, Henrys S, editors. *Antarctica at the close of a millennium*. Wellington, New Zealand: Bulletin of the Royal Society of New Zealand; p. 453–469.

Fleming TH, Foland KA, Elliot DH. 1999. Apophyllite 40Ar/39Ar and Rb-Sr geochronology: potential utility and application to the timing of secondary mineralization of the Kirkpatrick Basalt, Antarctica. *Journal of Geophysical Research*. 104:20,081–20,095.

Gerrish L, Fretwell P, Cooper P. 2020. Medium resolution vector contours for Antarctica (7.3) [Data set]. UK Polar Data Centre, Natural Environment Research Council, UK Research & Innovation. doi:10.5285/0779002b-b95d-432f-b035-b952c36aa5c9’.

Gleadow AJW, Fitzgerald PG. 1987. Uplift history and structure of the transantarctic mountains: new evidence from fission track dating of basement apatite’s in the Dry valleys area, southern Victoria land. *Earth and Planetary Science Letters*. 82:1–14. doi:10.1016/0012-821X(87)90102-6.

Golledge NR, Marsh OJ, Rack W, Braaten D, Jones RS. 2014. Basal conditions of two transantarctic mountains outlet glaciers from observation-constrained diagnostic modeling. *Journal of Glaciology*. 60:855–866. doi:10.3189/2014JoG13J131.

Goodge JW. 2020. Geological and tectonic evolution of the transantarctic mountains, from ancient craton to recent enigma. *Gondwana Research*. 80:50–122. doi:10.1016/j.gr.2019.11.001.

Granot R, Dyment J. 2018. Late Cenozoic unification of east and west Antarctica. *Nature Communications*. 9(1):3189. doi:10.1038/s4167-018-05270-w.

Grunow AM, Kent DV, Dalziel IWD. 1987. Mesozoic evolution of west Antarctica and the Weddell Sea Basin: new paleomagnetic constraints. *Earth and Planetary Science Letters*. 86:16–26.

Grunow AM, Kent DV, Dalziel IWD. 1991. New paleomagnetic data from Thurston island: implications for the tectonics of west Antarctica and Weddell Sea opening. *Journal of Geophysical Research*. 96:17935–17954.

Guo H, Zeitler PK, Idleman BD, Fayon AK, Fitzgerald PG, McDannell KT. 2021. Helium diffusion systematics inferred from continuous ramped heating analysis of transantarctic apatites showing age overdispersion. *Geochimica et Cosmochimica Acta*. 310:113–130. doi:10.1016/j.gca.2021.07.015.

Hambrey MJ, Webb P-N, Harwood DM, Krissek LA. 2003. Neogene glacial record from the Sirius Group of the Shackleton Glacier region, central Transantarctic Mountains, Antarctica. *Geological Society of America Bulletin*. 115:994–1015.

Harwood DM. 1986. Diatom biostratigraphy and paleoecology with a Cenozoic history of Antarctic Ice sheets. PhD dissertation, Ohio State University, p. 592.

He J, Thomson SN, Reiners PW, Hemming SR, Licht KJ. 2021. Rapid erosion of the central Transantarctic Mountains at the Eocene-Oligocene transition: evidence from skewed (U-Th)/He date distributions near Beardmore Glacier. *Earth and Planetary Science Letters*. 567:117009. doi:10.1016/j.epsl.2021.117009.

Howat IM, Porter C, Smith BE, Noh M-J, Morin P. 2019. The reference elevation model of Antarctica. *The Cryosphere*. 13:665–674. doi:10.5194/tc-13-665-2019.

Huerta AD. 2007. Byrd drainage system: evidence of a Mesozoic West Antarctic plateau. In: Cooper AK, Raymond CR, et al., editors. *A keystone in a changing world: Antarctica*. pp 1–5. On line proceedings of the 10th ISAES, U.S.G.S Open-File Report 2007- 1047, extended abstract 091, 5p. Washington DC: National Academy of Sciences.

Isbell JL. 1999. The Kukri Erosion Surface; a reassessment of its relationship to the rocks of the beacon supergroup in the central Transantarctic Mountains, Antarctica. *Antarctic Science*. 11:228–238.

Ives LRW, Isbell JL. 2021. A lithofacies analysis of a south polar glaciation in the early Permian: Pagoda formation, Shackleton Glacier region, Antarctica. *Journal of Sedimentary Research*. 91:611–635. doi: 10.2110/jsr.2021.004.

Katz HR. 1982. Post-Beacon tectonics in the region of Amundsen and Scott glaciers, Queen Maud Range, Transantarctic Mountains. In: Craddock C, editor. *Antarctic geoscience*. Madison, WI: University of Wisconsin Press; p. 827–834.

LaPrade KE. 1969. Geology of the Shackleton Glacier area, Queen Maud Range, Transantarctic Mountains, Antarctica. Ph.D. dissertation. Texas Technological College, Lubbock, Texas, 417 pp.

Lewis AR, Marchant DR, Ashworth AC, Hedenäs L, Hemming SR, Johnson JV, Leng MJ, Machlus ML, Newton AE, Raine JI, et al. 2008. Mid-Miocene cooling and the extinction of tundra in continental Antarctica. *Proceedings of the National Academy of Sciences*. 105:10676–10680.

Lindsay JF, Barrett PJ, Gunner JG. 1973. Reconnaissance geologic map of the Mount Elizabeth and Mount Kathleen Quadrangles, Transantarctic Mountains. United States Geological Survey. Washington DC: Antarctica 1:250,000 Map A-2.

Mayewski PA, Goldthwait RP. 1985. Glacial events in the Transantarctic Mountains: a record of the east antarctic Ice sheet. In: Turner MD, Splittstoesser JF, editors. *Geology of the central Transantarctic Mountains*. Washington DC: American Geophysical Union; Antarctic Research Series. 36:275–324.

Mayewski PA. 1975. Glacial geology and late Cenozoic history of the Transantarctic Mountains, Antarctica. Ohio State University, Institute of Polar Studies Report No 56, p. 168.

McGregor VR, Wade FA. 1969. Geology of the western Queen Maud Mountains. Geologic map of Antarctica, Sheet 16. New York: American Geographical Society.

McGregor VR. 1965. Notes on the geology of the area between the heads of the Beardmore and Shackleton Glaciers, Antarctica. *New Zealand Journal of Geology and Geophysics*. 8:278–291.

McKay RM, Barrett PJ, Levy RS, Naish TR, Golledge NR, Pyne A. 2016. Antarctic Cenozoic climate history from sedimentary records: ANDRILL and beyond. *Philosophical Transactions of the Royal Society*. A374:20140301. doi:10.1098/rsta.2014.0301.

Mercer JH. 1972. Some observations on the glacial geology of the Beardmore Glacier area. In: Adie RJ, editor. *Antarctic Geology and Geophysics*. Oslo: Universitetsforlaget; p. 427–433.

Miller SR, Fitzgerald PG, Baldwin SL. 2001. Structure and kinematics of the central Transantarctic Mountains:

constraints from structural geology and geomorphology near cape surprise. *Terra Antarctica*. 8:11–24.

Miller SR, Fitzgerald PG, Baldwin SL. 2010. Cenozoic range-front faulting and development of the Transantarctic Mountains near cape surprise, Antarctica: thermochronologic and geomorphologic constraints. *Tectonics*. 29: TC1003. doi:10.1029/2009TC002457.2010.

Passchier S, seven others. 2012. Early and middle Miocene Antarctic glacial history from sedimentary facies distribution in the AND-2A drill hole, Ross Sea, Antarctica. *Geological Society of America Bulletin*. 123:2352–2365. doi:10.1130/B30334.1.

Prentice ML, Denton GH, Lowell TV, Conway HC, Heusser LE. 1986. Pre-late quaternary glaciation of the Beardmore Glacier region, Antarctica. *Antarctic Journal of the United States*. 21(5):95–98.

Ryberg PE, Taylor EL. 2007. Silicified wood from the Permian and Triassic of Antarctica: tree rings from polar paleolatitudes. In: Cooper AK, Raymond CR, editors. *Antarctica: a keystone in a changing world*. Washington DC: National Academies Press. USGS OF-2007-1047, Short Research Paper 080, 5pp; doi:10.3133/of2007-1047.srp080

Shen W, Wiens DA, Stern T, Anandakrishnan S, Aster RC, Dalziel I, Hansen S, Heeszel DS, Huerta A, Nyblade A, et al. 2018. Seismic evidence for lithospheric foundering beneath the southern Transantarctic Mountains. *Geology*. 46:71–74. doi:10.1130/G39555.1.

Siddoway CS, Baldwin SL, Fitzgerald PG, Fanning CM, Luyendyk BP. 2004. Ross Sea mylonites and the timing of intracontinental extension within the West Antarctic rift system. *Geology*. 32:57–60. doi:10.1130/G20005.1.

Siddoway CS. 2008. Tectonics of the West Antarctic rift system: new light on the history and dynamics of distributed intercontinental extension. In: Cooper AK, Raymond CR, editors. *Antarctica: a keystone in a changing world*. Washington DC: National Academies Press; p. 91–114.

Smellie JL, Panter KS. 2021. Lithofacies and eruptive conditions of the southernmost volcanoes in the world (87° S). *Bulletin of Volcanology*. 83:49. doi:10.1007/s00445-021-01475-y.

Stern TA, Baxter AK, Barrett PJ. 2005. Isostatic rebound due to glacial erosion within the transantarctic mountains. *Geology*. 33:221–224. doi:10.1130/G21068.1.

Stump E, Borg SG, Sheridan MF. 1990a. Sheridan Bluff. In: LeMasurier WE, Thomson JW, editors. *Volcanoes of the Antarctic plate and southern oceans*. American Geophysical Union; Antarctic Research Series 48:136–137.

Stump E, Borg SG, Sheridan MF. 1990b. Mount Early. In: LeMasurier WE, Thomson JW, editors. *Volcanoes of the Antarctic plate and southern oceans*. Washington DC: American Geophysical Union; Antarctic Research Series 48:138–139.

Stump E, Sheridan MF, Borg SG, Sutter JF. 1980. Early Miocene subglacial basalts, East Antarctic ice sheet, and uplift of the Transantarctic Mountains. *Science*. 207:757–759.

Taylor EL, Cuneo R, Taylor TN. 1991. Permian and Triassic fossil forests from the central Transantarctic Mountains. *Antarctic Journal of the United States*. 26(5):23–24.

ten Brink US, Hackney RI, Bannister S, Stern TA, Makovsky Y. 1997. Uplift of the Transantarctic mountains and the bedrock beneath the East Antarctic ice sheet. *Journal of Geophysical Research*. 102:27,603–27,621. doi:10.1029/97JB02483.

Tinto KJ, Padman L, Siddoway CS, Springer SR, Fricker HA, Das I, Caratori Tontini F, Porter DF, Frearson NP, Howard SL, et al. 2019. Ross Ice shelf response to climate driven by the tectonic imprint on seafloor bathymetry. *Nature Geoscience*. 12:441–449.

van Wijk JW, Lawrence JF, Driscoll NW. 2008. Formation of the Transantarctic Mountains related to extension of the West Antarctic Rift system. *Tectonophysics*. 458:117–126. doi:10.1016/j.tecto.2008.03.009.

Wilson GS, Barron JA, Ashworth AC, Askin RA, Carter JA, Curren MG, Dalhuisen DH, Friedman EI, Fyodorov-Davidov DG, Gilichinsky DA, et al. 2002. The Mount Feather Diamicton of the Sirius Group: an accumulation of indicators of Neogene Antarctic glacial and climatic history. *Palaeogeography, Palaeoclimatology, Palaeoecology*. 182:117–131.

Wilson TJ. 1992. Mesozoic and Cenozoic kinematic indicators of the Transantarctic Mountains. In: Yoshida Y, Kaminuma K, Shiraishi K, editors. *Recent progress in Antarctic Earth Science*. Tokyo: Terra Scientific Publishing Company; p. 303–314.

Wilson TJ. 1993. Jurassic faulting and magmatism in the Transantarctic Mountains: implications for Gondwana break-up. In: Findlay RH, Unrug R, Banks MR, Veevers JJ, editors. *Gondwana eight-assembly, evolution, dispersal*. Rotterdam: AA Balkema; p. 563–572.